

Allorecognition in a Basal Chordate Consists of Independent Activating and Inhibitory Pathways

Tanya R. McKittrick,^{1,2} Christina C. Muscat,² James D. Pierce,¹ Deepta Bhattacharya,³ and Anthony W. De Tomaso^{1,*}

¹Department of Molecular, Cellular and Developmental Biology, University of California, Santa Barbara, Santa Barbara, CA 93106, USA

²Department of Biology and the Institute for Stem Cell Biology and Regenerative Medicine, Stanford University, Stanford CA 94305, USA

³Department of Pathology and Immunology, Washington University School of Medicine, St. Louis, MO 63110, USA

*Correspondence: detomaso@lifesci.ucsb.edu

DOI 10.1016/j.immuni.2011.01.019

SUMMARY

Histocompatibility in the basal chordate *Botryllus schlosseri* is controlled by the polymorphisms of a single gene: the *fuhc*. A polymorphic candidate receptor (*fester*) appeared to play roles in both initiating the reaction and discriminating between *fuhc* alleles. Here we report the characterization of a related protein, *uncle fester*. *uncle fester* is not polymorphic, and although coexpressed with *fester*, has different functional properties. Loss-of-function studies demonstrate that *uncle fester* was required for incompatible reactions but has no role in interactions between compatible individuals. Furthermore, stimulation with monoclonal antibodies could initiate a rejection phenotype on a single colony, and in both assays the severity of the rejection could be manipulated. These findings suggest that allorecognition in *Botryllus* consists of independent pathways that control compatible and incompatible outcomes that are integrated within the interacting cells, and may provide insight into basal processes conserved in allorecognition responses throughout the metazoa.

INTRODUCTION

Histocompatibility is the ability to discriminate self from nonself tissues, with examples found in nearly all metazoan phyla, from sponges to chordates (Burnet, 1971). This process is initiated by a natural or experimental mixing of tissues from different genotypes, which are either accepted, forming a chimera, or rejected, during which the interacting tissues are destroyed. This process ultimately relies on the discrimination of highly polymorphic ligand(s), but how specificity is achieved is not well understood. In vertebrates, allorecognition is a function of immunity and is mainly due to polymorphisms of the major histocompatibility complex (MHC) proteins, recognized by effector cells in both the adaptive (T cells) and innate (natural killer [NK] cells) branches of the immune system. However, despite the phenotypic similarities of allo-responses between higher vertebrates and other metazoans, there is no conservation of the ligands and receptors: orthologs of the MHC, T cell receptor, and NK

receptor genes cannot be found in jawless fish, lower chordates, or invertebrates, and candidate histocompatibility genes in species below the jawed vertebrates are not even homologous to each other, even within the same phylum (De Tomaso, 2009; Litman et al., 2010). Thus, although it is clear that the ability to discriminate between polymorphic histocompatibility ligands has an early evolutionary origin, the molecular and cellular basis of specificity and any potential conservation of this complex process remain enigmatic.

Botryllus schlosseri is a colonial ascidian with an experimentally accessible allorecognition system. Ascidiates are a group of basal chordates found in shallow marine habitats throughout the world (Delsuc et al., 2006). Embryogenesis results in a swimming chordate larva, which later settles and undergoes metamorphosis, resulting in a sessile invertebrate adult. *B. schlosseri* is also a colonial species and grows by a process of asexual budding, eventually resulting in a colony of genetically identical individuals (zooids) united by a common extracorporeal vasculature. The zooids and vasculature are embedded in a cellulose-based tunic, and the extracorporeal vasculature ramifies throughout this matrix and at the periphery terminates in finger-shaped projections called ampullae (example in Figure 3A).

When two colonies grow close together, the ampullae touch and initiate an allorecognition reaction that will result in either (1) a fusion of the juxtaposed vessels or (2) a rejection reaction which blocks parabiosis. The time from contact to a fusion or rejection reaction typically takes 24–48 hr and is limited to the ampullae in contact. Thus, a colony can simultaneously reject on one side and fuse on the other, suggesting that allorecognition is due to spatially restricted interactions and is not globally activated within the colonies.

Fusion or rejection is determined by the polymorphisms of a single protein, called the *fuhc* (De Tomaso et al., 2005): two colonies will fuse if they share one or both *fuhc* alleles and reject if no alleles are shared. Functionally, this is reminiscent of the missing-self recognition found in vertebrate NK cells (Kärre et al., 1986), and it has been shown that this recognition event is highly discriminatory. The *fuhc* gene is highly polymorphic and the effector system can recognize a self-*fuhc* allele from hundreds to potentially a thousand competing alleles (Scofield et al., 1982; Rinkevich et al., 1995). However, the molecular and cellular basis of this discriminatory ability is unclear. In a previous report we identified another protein encoded near the *fuhc*, called *fester*, that appears to be a receptor in this reaction (Nyholm et al., 2006). *fester* is also highly polymorphic, but these polymorphisms do not correlate to fusion or rejection

outcomes: colonies sharing an allele can reject and those sharing neither can fuse. However, two *in vivo* assays suggested that *fester* was a receptor in this reaction. First, when a monoclonal antibody (mAb) raised to a *fester* was injected into incompatible colonies as they came into contact, the ampullae fused instead of rejecting. This suggested that *fester* was a receptor for the *fuhc* and responsible for discriminating between different alleles and that mAb binding mimicked binding to a self-*fuhc* allele. In contrast, siRNA-mediated knockdown of *fester* rendered the ampullae unreactive, and they would neither fuse nor reject, suggesting that an activating phase of histocompatibility existed and that *fester* was also involved in this phase of recognition (Nyholm et al., 2006). However, at that point it was unclear whether fusion and rejection was akin to an on or off reaction (i.e., a rejection needed to be activated for a fusion to occur) or whether *fester* was an integral part of two pathways, one controlling activation and one controlling fusion.

We have identified a nonpolymorphic member of the *fester* family encoded within 50 kb of the *fester* locus that has revealed a functional separation of fusion and rejection pathways. This protein is coexpressed with both *fester* and the *fuhc* and was involved in initiating the rejection response between incompatible colonies, but had no role in compatible interactions. This finding demonstrates that two independent pathways control histocompatibility in *B. schlosseri*, providing insight into the mechanisms of specificity.

RESULTS

Genetic Mapping, Cloning, and Sequencing of a New *fester* Family Member

Mining of the genomic sequence database encompassing the *fuhc* locus (De Tomaso and Weissman, 2003) revealed a duplication of part of the *fester* gene encoding exons 6–11 but with no homology to exons 1–5 or to the secretory exon (exon 12). This duplicated region, located between the *fester* and *fuhc* loci, was 30 kb in length and >90% identical to *fester* at the nucleotide level in both exon and intron sequences (Figure S1 available online). Primers were designed from this sequence and a cDNA clone was isolated by RACE that encodes a predicted transmembrane protein that is structurally identical to the full-length *fester* protein, and contained a signal sequence, extracellular SCR domain, three contiguous transmembrane helices, and a short intracellular tail (Figure S1). The gene consists of nine exons spanning a genomic region of ~46 kb, and the last five exons encode two predicted extracellular and the three transmembrane domains that are nearly identical to the full-length *fester* A-clade allele (exons 6–11) at the amino acid level (Figure S1; Nyholm et al., 2006). However, the majority of the extracellular domain (exons 1–3), including the SCR domain found in exon 3, is completely distinct from the corresponding region of the *fester* locus. Because of the structural and nucleotide similarity to *fester* and the 50% homology, this gene is being called *uncle fester*. Besides the SCR domain, *uncle fester* is not related to any other proteins found in the database or within the complete genome sequence of a related ascidian (Azumi et al., 2003; Dehal et al., 2002).

Despite these similarities and its close physical proximity to both the *fuhc* and *fester* loci, we found that *uncle fester* is not

polymorphic at either the nucleotide or amino acid level. Sequences were nearly identical within and among all populations sampled on the west coast of North America (Table S1). Only two silent single-nucleotide polymorphisms (SNPs) and an amino acid deletion were found in east coast populations, and these polymorphisms were found to be segregating within this population (Table S1). These findings were in sharp contrast to the unusually high degree of polymorphism found in the closely related *fester* gene as well as the *fuhc* (De Tomaso et al., 2005; Nyholm et al., 2006).

Expression Profile of *uncle fester*

uncle fester expression was initially characterized at different stages of embryogenesis by RT-PCR (Figure 1). Expression was first detected in the early stages of embryonic development (the tailbud stage) and continues throughout the life cycle of the individual (Figure 1A). These studies also revealed that *uncle fester* was alternatively spliced in both the embryo and adult, although to a much lesser degree than *fester*. Each adult examined thus far expressed three variants of *uncle fester*: a full-length transcript, a splice variant eliminating exon 5, and another without exons 4 and 5. *uncle fester* exons 4 and 5 correspond to *fester* exons 6 and 7, respectively, and are the most commonly spliced exons in the *fester* mRNA (Figure S1). These three variants migrated as a single band in Figure 1A (top arrow; see Experimental Procedures).

In addition, we also found that embryos and tadpoles expressed an additional set of splice variants, which removed exons 2 and/or 3 as well as the same combinations of exons 4 and 5 (Figure 1A, bottom arrow; these variants also comigrate). In summary, three variants are expressed at all times, while another six appear to be expressed exclusively during embryogenesis (Figure 1A). The role of these splice variants is unknown.

uncle fester mRNA localization was determined by *in situ* hybridization by means of a probe specific to the *uncle fester* transcript (exons 1–3), which would detect all splice variants. In the tadpole larvae, expression of *uncle fester* was restricted to the developing ampullae (Figure 1B), as well as in structures called the adhesive papillae (Figure 1C). In both the oozoids and adults, expression was limited to the epithelia of the ampullae and a subset of blood cells both within the vasculature and within the tunic matrix (Figure 1D).

We also created mAbs to the full-length *uncle fester* protein as previously described (Nyholm et al., 2006). Two mAbs were isolated (2b6 and 5d9) that recognized the full-length and both adult splice variants of *uncle fester* by both flow cytometry and immunofluorescence (IF) when expressed in mammalian cells, but had no reactivity to full-length *fester* (Figures S2F and S2G). In addition, the *fester* antibody (5b1) did not react to the full-length *uncle fester* protein (Nyholm et al., 2006). We used these mAbs to characterize protein expression by IF (Figures 1H–1J). Results from both mAbs were equivalent and showed that protein expression was completely concordant with mRNA localization, with *uncle fester* protein identified on the epithelia of the ampullae and a subset of blood cells both within the vasculature and within the tunic matrix.

Previous studies have shown that *fester* is also expressed along the epithelia of the ampullae as well as a subset of blood cells in the vasculature and tunic. However, comparison of *fester*

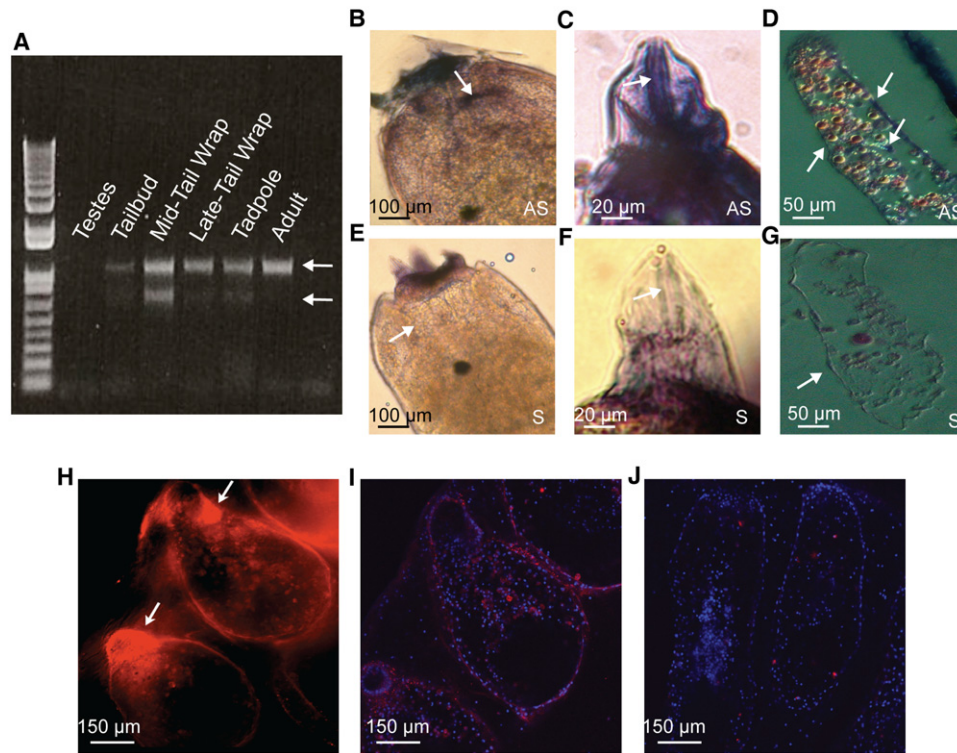


Figure 1. Expression of *uncle fester*

(A) Expression of *uncle fester* by RT-PCR in testes and during defined stages of embryogenesis (tailbud, mid-tail wrap, and late-tail wrap), tadpole larvae, and adult. Changes in splice variant expression can be seen during this time. The top arrow points to a band in which the three variants that are expressed in all stages comigrate. The bottom arrow points to the variants expressed exclusively during embryogenesis and in the larva (which also comigrate in agarose gels) (see [Experimental Procedures](#)).

(B–G) In situ hybridization of *uncle fester* in tadpoles and adults. Antisense probes shown in (B), (C), and (D); sense control probes shown in (E)–(G).

(B) Expression of *uncle fester* is seen on the developing ampullae (arrow) in the head of the tadpole larvae.

(C) Expression is also observed in nerves running through the larval adhesive papillae located at the anterior portion of the tadpole (arrow).

(D) Histological sections of adult ampullae. *uncle fester* is expressed along the epithelia of the ampullae (outside arrows) and a subset of blood cells (arrow inside ampullae).

(E) Positive control of (B). There is nonspecific background on the anterior end, but nascent ampullae are not stained (arrow).

(F) Positive control of (C); there is no staining along the ampullar nerves (arrow).

(G) Positive control of (D); there is no staining on the epithelium of the ampullae (arrow).

(H–J) Whole-mount and confocal IF via *uncle fester*-specific monoclonal antibodies showing protein expression in adult colonies (red); samples were counterstained with DAPI (blue).

(H) Whole-mount images of adult ampullae; expression is seen on the tips of the ampullae (arrows).

(I) Confocal images of adult ampullae.

(J) Secondary only control.

All experiments were repeated a minimum of four times.

([Nyholm et al., 2006](#)) and *uncle fester* expression patterns ([Figures 1H and 1I](#)) also suggested that there were many more *fester*⁺ cells in the tunic. To directly assess coexpression of the two proteins, we carried out both double-labeled flow cytometry and IF analysis with directly conjugated *fester* and *uncle fester* mAbs. For the former, dissociated cell preparations from whole colonies were isolated and analyzed, and as shown in [Figure 2E](#), all cells that express *uncle fester* also expressed *fester*, and in addition there is a population of *fester*⁺*uncle fester*[−] cells.

To localize the two populations, we analyzed whole-mount colonies by double-labeled IF ([Figures 2A–2C](#)). We found that the epithelia of the ampullae and a subset of cells in the circulation were double labeled ([Figures 2B and 2C](#)), whereas both *fester*⁺*uncle fester*⁺ ([Figures 2B and 2C](#), red arrows) and *fester*⁺*uncle*

fester[−] ([Figures 2B and 2C](#), white arrows) cells were found in tunic. A good comparison of the two populations in the vasculature was difficult to assess because of pigment cells in the blood, which are autofluorescent with these techniques ([Figure 2D](#)), but whole-mount analysis was necessary to see cells that are embedded within the cellulose-based tunic matrix that is ~1 mm thick. In summary, flow cytometry analysis suggests that all *uncle fester*⁺ cells were also *fester*⁺, and IF results confirmed that this was true along the epithelium of the ampullae, the site of allorecognition. In addition, there appears to be a mobile population of *fester*⁺*uncle fester*⁺ and *fester*⁺*uncle fester*[−] cells that migrate into the tunic matrix. The role of these mobile cells is unknown.

An observation from the flow cytometry analysis was a nearly linear relationship between the expression of the two proteins on

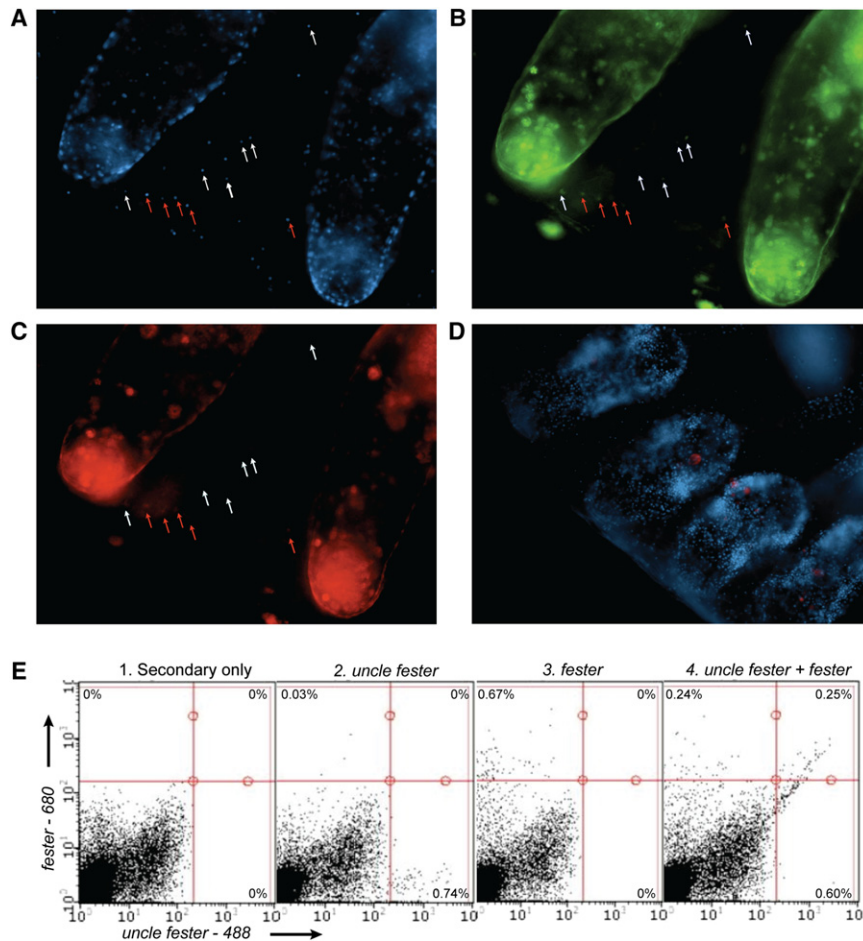


Figure 2. Coexpression of *fester* and *uncle fester*

(A–C) Whole-mount immunofluorescence via directly conjugated mAbs to *fester* and *uncle fester*.

(A) DAPI staining of (B) and (C) showing cells in tunic between two ampullae (red and white arrows).

(B) *fester* expression in the same field. Epithelia of the ampullae and cells in the vasculature and tunic matrix are *fester*⁺ (red and white arrows).

(C) *uncle fester* expression in the same field. Epithelia of the ampullae, cells in the vasculature, and in the tunic are labeled. In the tunic, both *fester*⁺*uncle fester*⁺ cells (red arrows) and *fester*⁺/*uncle fester*⁻ cells (white arrows) are present.

(D) Overlay of secondary only control via mouse anti-IgG 488 and mouse anti-IgG 594 alone, counterstained with DAPI (blue). Note that autofluorescence of pigment cells in the vasculature can be seen in both 488 and 594 channels in these whole-mount images.

(E) Flow cytometry analysis of *Botryllus* cells counterstained with (1) both mouse anti-IgG 488 and mouse anti-IgG 680 alone as a secondary control, (2) *uncle fester* mAb conjugated with Dylight-488, (3) *fester* mAb conjugated with Dylight-680, and (4) both *uncle fester*-488 and *fester*-680.

the double-labeled cells (Figure 2E). Because the antibodies do not cross react (Figure S2; Nyholm et al., 2006), it seems unlikely that this correlation was an artifact. This suggests that expression of *uncle fester* and *fester* is regulated in those cells, and as described below, is consistent with functional analysis.

***uncle fester* Initiates the Rejection Reaction**

The function of *uncle fester* was determined in vivo by two different experimental procedures. First, we used a previously described in vivo assay that links siRNA-mediated knockdown to vascular regeneration (Nyholm et al., 2006), called an ampullactomy. Second, ampullae were directly stimulated with mAbs linked to magnetic beads.

For the former, we had previously found that when the entire extracorporeal vasculature is surgically removed, it will regenerate within 72 hr and the newly developed ampullae are capable of undergoing *fuhc*-based allorecognition with no loss of specificity. When regeneration takes place under conditions of siRNA-mediated knockdown of genes expressed in the ampullae, they will regenerate without the corresponding protein (Nyholm et al., 2006). After regeneration, colonies are placed into contact and histocompatibility phenotypes assessed. Knockdown of the gene is then confirmed via qPCR analysis of the

isolated ampullae and phenotype correlated to expression levels. The colonial nature of *B. schlosseri* is a convenient characteristic for these studies, because an individual can be cut into multiple pieces (subclones), which will continue to grow. Thus multiple experiments can be done on a single genotype, and the controls for these experiments are subclones of the same genotypes, which are subjected to siRNA treatment to a non-*Botryllus* protein (GFP). Another control was to determine whether *uncle fester* knockdown had any effect on the expression of the *fester* protein. As shown in Figure 3A, *fester* is still expressed on the ampullae of individuals that lack *uncle fester* expression.

Both fusion and rejection reactions begin with an inflammatory reaction, whereby a refractile hemocyte called a morula cell migrates to the tips of the interacting ampullae (Cima et al., 2004). If the colonies are incompatible, the epithelia of the ampullae become leaky, and the morula cells migrate into the region between the ampullae and burst open, releasing the precursors of a prophenoloxidase pathway (Ballarin et al., 1995; Rinkevich et al., 1998), which eventually results in the formation of dark melanin scars called points of rejection (POR). In contrast, if colonies are compatible, morula cells are not released, and the opposing ampullae initiate a vascular remodeling pathway, which results in fusion of the juxtaposed vessels. The allorecognition response is restricted to the ampullae in contact, and a colony can simultaneously reject on one side and fuse on the other.

In the first set of experiments, incompatible colonies were paired in which both were treated with *uncle fester*-specific

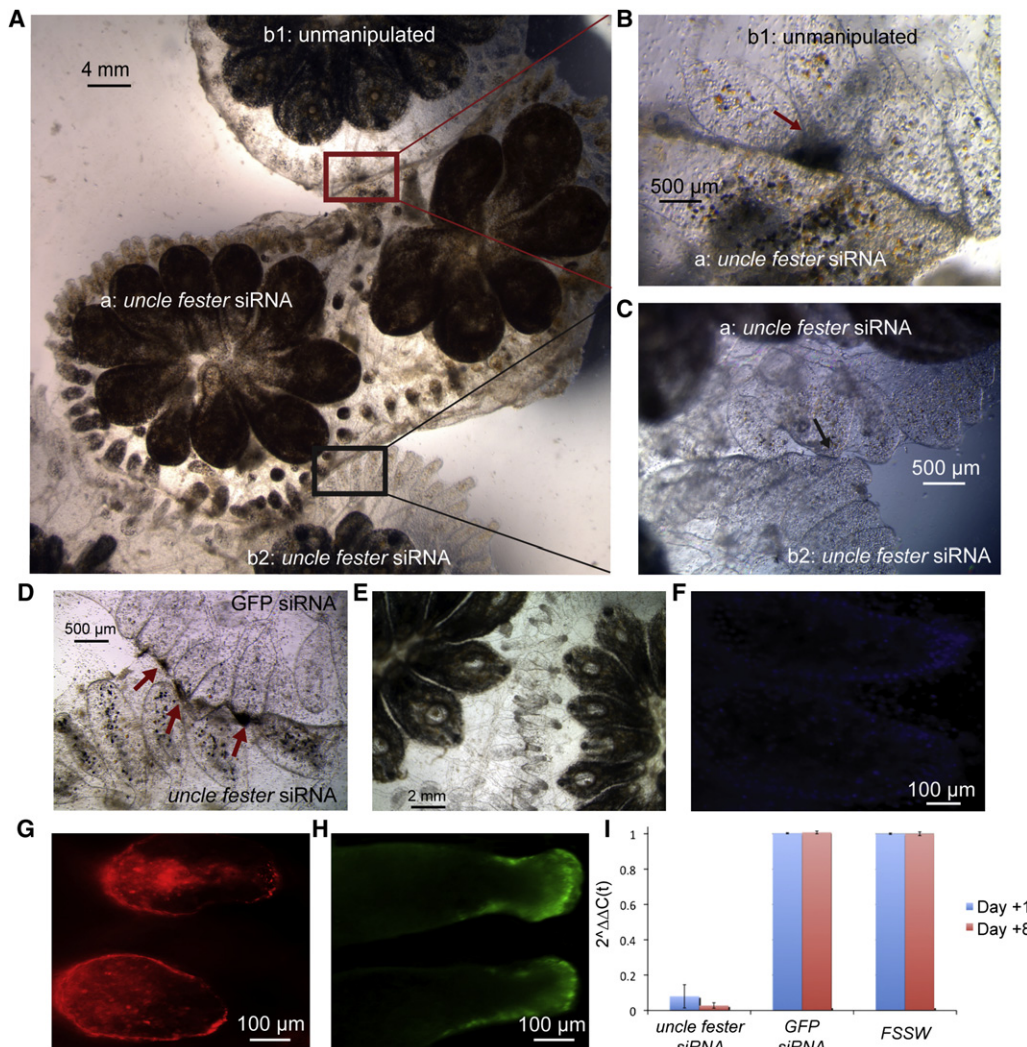


Figure 3. siRNA Knockdown of *uncle fester*

(A) Three-way interaction between two identical colonies (b1 and b2) and an incompatible colony (a). Both colonies a and b2 are under the effects of *uncle fester* siRNA, whereas colony b1 is unmanipulated. Colony b1 rejects colony a within 48 hr, whereas colonies a and b2 are not reacting.

(B) Close up of the interaction between a and b1 in (A) showing clear POR between the unmanipulated and *uncle fester* knockdown genotype.

(C) Close-up of the interaction between colony a and b2 in (A). Ampullae in both colonies do not show normal inflammation for 96 hr after contact.

(D) A colony under GFP siRNA (top) shows swelling and POR when placed in contact with a colony under *uncle fester* knockdown (bottom).

(E) 24 hr after histocompatible colonies under the effects of *uncle fester* siRNA come into contact. Ampullae rapidly penetrate the tunic, swell, and initiate fusion on the same time course as the controls.

(F) A colony treated with *uncle fester* siRNA and counterstained with *uncle fester* mAb (red) and DAPI (blue).

(G) A colony treated with GFP siRNA and counterstained with *uncle fester* mAb (red).

(H) A colony treated with *uncle fester* siRNA and counterstained with *fester* mAb (green). *fester* is expressed in ampullae even though *uncle fester* expression is absent.

(I) qPCR of samples treated with *uncle fester* siRNA, GFP siRNA, and filtered sterile seawater (FSSW). Relative expression of *uncle fester* under knockdown normalized to control conditions is shown (see [Experimental Procedures](#)).

siRNA (Table 1). Under these conditions we observed a “no-reaction” phenotype, during which the ampullae came into contact but did not display the typical inflammation, nor did they develop any PORs for up to 5 days after initial contact (Table 1; phenotype shown in Figure 3C), replicating the *fester* knockdown (Nyholm et al., 2006). In contrast, control subclones reacted normally within 48 hr, showing typical inflammation and POR formation. Analysis by qPCR of isolated ampullae after

the 5 days of interaction demonstrated that *uncle fester* transcript was 99.9% depleted during the experiment, whereas expression in control subclones was unaffected (Figure 3I). In addition, *uncle fester* protein expression was not detected via IF in colonies after knockdown, and there was no effect of *uncle fester* siRNA on *fester* protein (Figure 3H) or mRNA expression (not shown). In summary, *uncle fester* is necessary to initiate the rejection response, as we had previously found for *fester*

Table 1. siRNA-Mediated Knockdown of *uncle fester*

Treatment	Compatibility	Outcome (Rejection/ Fusion/No Reaction)
UF siRNA versus UF siRNA	incompatible	0/0/5
UF siRNA versus UF siRNA (partial knockdown)	incompatible	8/0/0
UF siRNA versus GFP siRNA	incompatible	3/0/0
GFP siRNA versus GFP siRNA	incompatible	3/0/0
UF siRNA versus UF siRNA	compatible	0/9/0
UF siRNA versus GFP siRNA	compatible	0/5/0
GFP siRNA versus GFP siRNA	compatible	0/3/0

Loss-of-function assays were carried out as described in the text. *fuhc*-genotyped individuals were subjected to siRNA treatment during vascular regeneration and paired to a compatible or incompatible partner, and outcome (fusion, rejection, or no reaction) was visually assessed. Replicates and number of observations in each class are shown. Unless stated, knockdown of *uncle fester* blocked 99% of normal expression.

(Nyholm et al., 2006). In both experiments, siRNAs were designed to knock down all splice variants, and given the coexpression of the two proteins on the same population of cells in the ampullae (Figure 2), we hypothesize that a combination of full-length and/or common splice variants of the two proteins may form a heterodimeric receptor that is responsible for initiating the rejection reaction, and this is being tested now.

Next we asked whether a threshold of *uncle fester* expression existed that could still initiate a rejection reaction, and we varied siRNA concentrations such that knockdown would be less severe (see Experimental Procedures). At 50% knockdown, no effect was observed, and *uncle fester* knockdown colonies rejected with the same kinetics as controls (Table 1). When 95% of the *uncle fester* transcript was depleted, most of the ampullae remained unreactive, but in two cases a single POR developed along the interface after more than 5 days of contact (versus 2 days for POR formation in controls; not shown). Thus it appears that *uncle fester* expression levels correlate to both the presence and the severity of the rejection reaction.

In the next set of experiments, we asked whether the rejection reaction required the participation of both colonies, and we paired a control colony to an *uncle fester* knockdown colony. Within 24 hr of contact, ampullae from the control colony began to exhibit a typical rejection response, with morula cell infiltration and development of PORs within 48 hr (Table 1; Figure 3D, red arrows). In contrast, the colony under *uncle fester* knockdown remained unreactive. qPCR analysis revealed that the knockdown colony had <0.1% *uncle fester* expression, whereas the control showed normal levels. This suggested that a single colony could be stimulated to undergo a phenotypic rejection reaction and further that *uncle fester* is not involved in homotypic binding.

To confirm this one-way rejection phenotype, a 3-way assay was performed (Figure 3A) where two subclones of one genotype (b1 and b2) were simultaneously placed into contact on either side of an incompatible colony (a). The colony (b1) at the

top of Figure 3A was unmanipulated, while the colony in the center (a) and on the bottom (b2) are both under the *uncle fester* knockdown. After 4 days of contact, the unmanipulated colony (b1) has developed several PORs (Figure 3B), whereas the subclone on the other side with *uncle fester* knockdown remained unreactive, recapitulating previous results in a two-way pairing (Figure 3C). These results confirm the one-way rejection phenotype between manipulated and unmanipulated colonies in single pairings. They also suggest that recognition occurs on the ampullae but that the phenotypic rejection is downstream of this recognition event and not due to direct allogeneic interactions between the morula cells that form the POR. This is directly tested in experiments shown in Figure 4 (described below).

uncle fester Plays No Role in the Fusion Reaction

We next tested the role of *uncle fester* between compatible colonies. When two compatible colonies, each under *uncle fester* knockdown, are placed into contact under the effects of the *uncle fester* siRNA, colonies exhibit a typical fusion response: the ampullae rapidly penetrate through the tunic and come into contact at the base of the peripheral vasculature, swell, and fuse within 24–48 hr after contact, equivalent to controls (Table 1; Figure 3E). If an *uncle fester* knockdown colony was paired to a control colony, there was also no effect on the fusion process (Table 1). In all experiments, *uncle fester* mRNA expression was >99.8% depleted and no protein expression could be seen by IF, and *fester* expression was unaffected (Figures 3F–3H). These results demonstrate that fusion does not require *uncle fester* expression and suggests that fusion and rejection are not outcomes of a single process that occurs upon interaction of the ampullae, but rather independent pathways: one responsible for inflammation and epithelial breakdown causing a rejection, the other for a vascular remodeling pathway resulting in a fusion. Interestingly, whereas *uncle fester* knockdown blocked the typical inflammation during the rejection response (Figure 3C), in compatible colonies the inflammation still occurred prior to fusion (Figure 3E), suggesting that there are two independent inflammatory pathways.

Stimulation of a Rejection In Vivo via mAbs

Concurrently we tested the ability of our *uncle fester* mAbs to alter histocompatibility reactions. As described in the methods, two *uncle fester* mAbs were produced that showed equivalent binding by IF and flow cytometry. These antibodies (5d9 and 2b6), as well as a control antibody that shows ubiquitous reactivity and appears to bind to the tunic (Nyholm et al., 2006), were independently bound to magnetic beads, and the beads were then placed into contact with the ampullae. This was done by placing a magnet underneath the glass slide in which the colony was attached and drawing the beads to the ampullae (Figure 4A). The beads were left on the ampullae for 10 min and then removed, and ampullae were visually monitored for the next 48 hr.

Although both the control mAb and *uncle fester* 5d9 mAb had no effect on the ampullae (Figure 4D), contact with 2b6 initiated a mild to severe rejection response that was dependent on the amount of beads applied (Table 2). When 5 μ l of beads were used, the ampullae began to swell and turn brown after 24 hr (Figure 4B). However, when 20 μ l of beads were applied, the

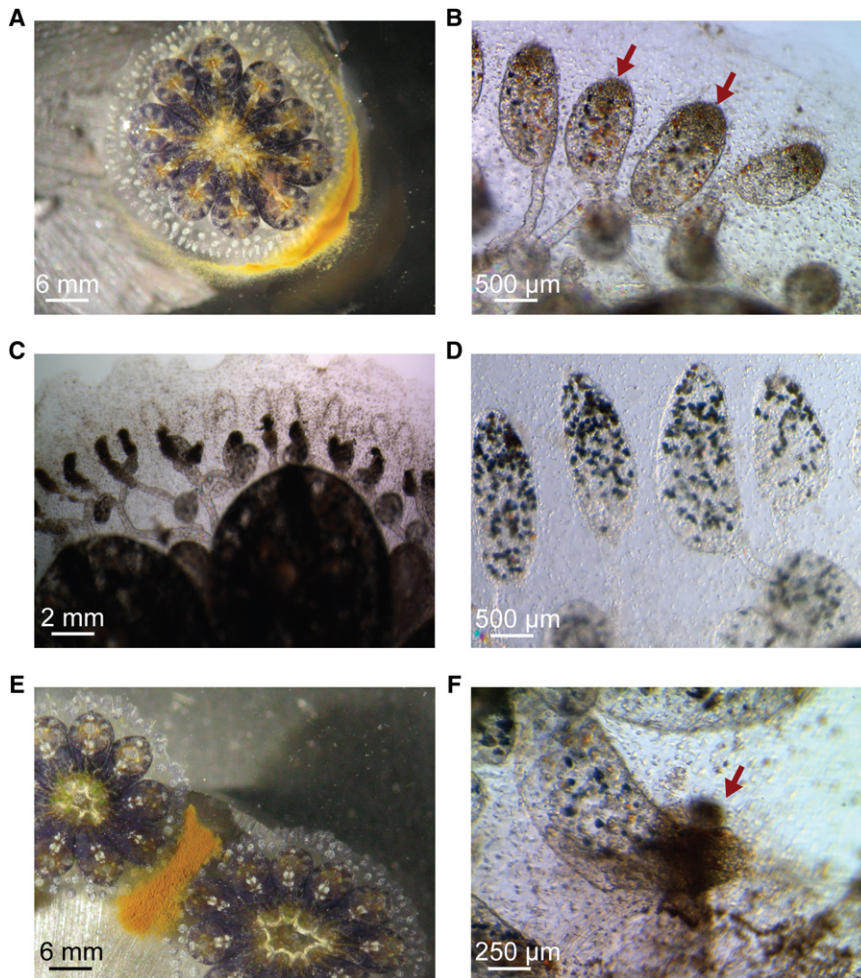


Figure 4. mAb Stimulation of *uncle fester* Initiates a Rejection Response

(A) Application of magnetic beads to the ampullae. (B) 5 μ l of magnetic anti-mouse IgG beads bound to *uncle fester*-specific mAb 2b6 were applied to the tips of the ampullae for 10 min. 24 hr later, the ampullae are swollen with morula cells and have begun to turn brown (red arrows; compare to D). (C) 20 μ l of magnetic anti-mouse IgG beads bound to mAb 2b6 were applied to the tips of the ampullae for 10 min. 24 hr later, every ampullae that was exposed to the mAb had completed a severe rejection response, with full amputation of several ampullae. (D) 24 hr after removal of magnetic beads bound to *uncle fester*-specific mAb 5d9. No characteristics of rejection are observed. (E) Bound mAb 2b6 added to a compatible pairing after contact but prior to fusion. (F) Close-up of the same ampullae 24 hr later. POR form on the tips of ampullae and no fusion is observed.

If integration of two independent pathways exists in *B. schlosseri*, then it should be possible to overstimulate the rejection pathway and override a fusion response. To initially test this hypothesis, we repeated this experiment with compatible colonies in which the ampullae had already come into contact but had not yet fused. We used the magnet to manipulate the beads so they were in contact only across the zone of interaction between the juxtaposed ampullae (Figure 4E). After removal of the beads, PORs developed rapidly

along the interface, the ampullae disassociated, and no fusions occurred (Figure 4F). Within 1 week after the beads were removed, the colonies naturally interacted again and fused. Thus on a global level, overstimulation of the rejection pathway can block a fusion reaction already in progress. However, these results do not provide specific information on what occurs in the cells at the tip of each ampulla. For example, it could be that POR formation from ampullae that were not in contact could sterically hinder the vascular remodeling of adjacent ampullae in contact that would have normally fused. Nevertheless, it is clear that on a global level, overstimulating the rejection reaction can prevent a fusion from occurring. Importantly, this is further evidence that fusion and rejection are distinct pathways, because initiation of fusion does not preclude a rejection response.

colony initiated a severe rejection response, with each ampullae that came into contact with the beads developing a POR, and in some cases completely amputating within 24 hr (Figure 4C; Table 2). The latter responses were more rapid and severe than rejection responses typically seen with two individuals, but in all cases swelling and POR development occurred only at the site of contact with beads bound to mAb 2b6 (Figure 4C versus 4D). The time lag between the transient mAb application and inflammation and POR formation confirms that the phenotypic rejection is downstream of *uncle fester* stimulation.

In summary, both loss-of-function and mAb stimulation demonstrate that *uncle fester* is necessary to initiate the rejection pathway. However, the fusion pathway is clearly not dependent on stimulation of the rejection pathway, because *uncle fester* knockdowns have no effect on compatible interactions. Given that *fester* and *uncle fester* are both expressed in the same population of cells at the tips of the ampullae, these results suggest that under normal conditions, binding of a self *fuhc* allele blocks the rejection pathway and initiates a vascular remodeling pathway, which results in fusion. In turn, fusion or rejection is probably determined via an integration of two signal transduction pathways, analogous to effector function in vertebrate immunity (Lanier, 2001).

DISCUSSION

B. schlosseri has an effector system that can discriminate between 100 and 500 alleles of a single protein, the *fuhc*. However, the basal chordates do not have the genome diversification toolkit (e.g., RAG or AID) to create allele-specific, high-affinity receptors from germline-encoded genes (Litman et al.,

Table 2. *uncle fester* mAb Stimulation Specifically Induces a Rejection Reaction on a Single Colony

Treatment	Swelling	Points of Rejection
<i>uncle fester</i> mAb: 2b6 5 μ l	6/6	3/6
<i>uncle fester</i> mAb: 2b6 20 μ l	5/5	5/5
<i>uncle fester</i> mAb: 5d9 20 μ l	0/5	0/5
nonspecific mAb: 1H3 20 μ l	0/5	0/5
beads alone 20 μ l	0/3	0/3

Antibodies were bound to magnetic beads and applied to the ampullae as described in the [Experimental Procedures](#). Beads (μ l) were in contact with the ampullae for 10 min and then removed, and the phenotype was visually assessed over the next 72 hr.

2010; Azumi et al., 2003). How does an innate recognition system differentiate between highly polymorphic ligands? An analogous situation exists in mammalian NK cells, where inhibitory receptors recognize polymorphic residues on MHC class I molecules in a missing-self reaction. Specificity is achieved via an education process during which receptors are stochastically expressed from an unlinked, multigenic locus encoding multiple (~8–40) polymorphic receptors, until one or multiple receptors that bind self-MHC alleles are expressed and a signaling threshold is achieved (Höglund and Brodin, 2010). After education, mature NK cells function via a balance of stimulatory and inhibitory signaling, and effector output (killing or tolerance) is determined by upregulation of activating ligands and/or downregulation of inhibitory ligands on target cells. Interestingly, this balance of activating and inhibitory function is also evident in the education process itself. Some NK cells never express an inhibitory receptor specific for a self-MHC allele and are hyporesponsive (Fernandez et al., 2005; Kim et al., 2005). In addition, NK cells that express multiple MHC class I-specific inhibitory receptors have significantly stronger responses to activation compared to those that express only a single inhibitory receptor (Brodin et al., 2009; Joncker et al., 2009).

Allorecognition in *B. schlosseri* also appears to be based on a balance between two independent pathways. Previously, we found that mAb binding to a single protein (*fester*) could override a rejection reaction in progress and initiate a fusion in vivo (Nyholm et al., 2006), suggesting that it was analogous to a mammalian inhibitory receptor, recognizing a self *fuhc* allele and blocking a default rejection reaction. In contrast, knockdown of *fester* rendered the ampullae unreactive in both compatible and incompatible pairings, suggesting the existence of an independent pathway that initiated a rejection response. The latter results were not surprising: ampullae do not react when they touch inert objects or other species, and we speculated that *fester* function was partitioned to the two pathways via intracellular splice variants that removed combinations of exons 9 and 10 and that these exons encoded domains involved in assembly with adaptor molecules encoding different signaling domains (Nyholm et al., 2006). However, these results provided no insight into the relationship of the two processes, specifically if the two pathways are functionally linked, such that a rejection needs to be initiated for a fusion to occur, or if they are independent and signals integrated in the ampullae, analogous to a balance of inputs which underlies effector outcome in vertebrate NK cells. Functional analysis of

uncle fester has allowed us to delineate the fusion and rejection pathways: knockdown of *uncle fester* blocks a rejection from occurring but has no effect on a fusion response, demonstrating that fusion and rejection are two independent pathways. Given that knockdown studies demonstrate that both *fester* and *uncle fester* are necessary to initiate a rejection reaction and that expression of the two proteins appears to be correlated, we hypothesize that *uncle fester* may be heterodimerizing with a common *fester* splice variant, forming a receptor responsible for initiating the rejection reaction, and this is currently being tested.

In addition, knockdowns and mAb interference experiments of both proteins provide solid evidence that the decision to fuse or reject is based on a balance between these two independent pathways. First, the severity of the rejection can be manipulated by changing the level of *uncle fester* knockdown or the strength of mAb stimulation; second, stimulation of one pathway with mAbs can override the other in progress.

A balance between fusion and rejection pathways was also suggested in a previous study on *B. schlosseri*, which was focused on understanding a well-documented variability in the severity of the rejection reaction. When individuals are randomly paired, four distinct rejection phenotypes can be observed (Nagashima and Scofield, 1981; Scofield and Nagashima, 1983). These phenotypes range from only slight bleeding and barely visible POR to rapid (<24 hr) POR production and ampullae disintegration, with two distinct intermediate states. Segregation of these phenotypes was analyzed in a series of crosses and it was found that the severity of the rejection response segregated with the *fuhc* locus; however, the molecules and mechanisms underlying recognition were unknown at that point (Scofield and Nagashima, 1983).

Subsequent genetic mapping of the *fuhc* locus suggested a role of the *fuhc* gene itself in the severity of the rejection response, because the only ambiguous scores for fusion or rejection in our mapping crosses occurred between two *fuhc* homozygotes (*fuhc AA* versus *fuhc BB*), pairings that showed almost no visible signs of rejection. This was not due to *fuhc* homozygosity because *fuhc AA* versus *YY* genotypes in the exact same genetic background (and often subclones of the same individuals) displayed severe rejections within 24 hr of contact. Interestingly, the *fuhc A* and *B* alleles are the least different, with 20 residue differences between them, whereas *fuhc A* and *Y* had 48 differences (De Tomaso et al., 2005; De Tomaso and Weissman, 2003). Importantly, both *fuhc A* and *Y* are linked to an equivalent *fester* allele, whereas *fuhc B* is linked to a completely divergent *fester* clade; thus, *fester* could not be directly involved in this response. Prior to the discovery of *uncle fester*, we had suggested that the most parsimonious explanation for the differences between *fester* mAb interference (suggesting that it was a *fuhc* receptor) versus knockdown (suggesting that it was involved in activation of the rejection) outcomes is that the *fuhc* is the ligand for both pathways (Nyholm et al., 2006). If so, the relationship between the severity of the rejection and the *fuhc* allele could be interpreted as closely related *fuhc* alleles partially mimicking each other and initiating an incomplete inhibitory response, weakening the severity of the rejection. Conversely, activation of the rejection reaction may be lower in these pairings, with similar alleles stimulating a weaker rejection, or it could be a combination of both processes.

A dual role of the *fuhc* is also consistent with the hypothesis that rejection is initiated through a *fester-uncle fester* heterodimeric receptor and would not be surprising, because the MHC can be both an activating and inhibitory ligand for vertebrate NK cells.

In either case, similar *fuhc* alleles would stimulate a weaker rejection, and indeed a potential role for the *fuhc* as a ligand for both rejection and fusion has complicated the interpretation of knockdown studies of this protein (data not shown). Nevertheless, as the polymorphisms of a single protein determine fusion and rejection outcome in *Botryllus*, we can now directly test these hypotheses in vivo, correlating rejection responses to *fuhc* polymorphisms. This will allow us to potentially pinpoint regions of the protein that are important for stimulating a rejection and/or generating new specificities, as well as directly assessing the sensitivity of the effector system.

In both the NK cell recognition of polymorphic residues of the MHC in the vertebrates, as well as recognition of the *fuhc* in *Botryllus*, polymorphism of the receptors is an order of magnitude less than that of the ligand. This is inconsistent with a lock and key mode of recognition and implies that specificity is achieved in an alternative manner, most probably by an overall avidity from multiple binding events at the cell surface. The ability to generate specificity by this type of recognition requires that the effector system have two properties. First would be a mechanism to quantify binding avidity, coupled to a preset signaling threshold. Second would be a process to generate diversity of the germline-encoded receptors on the cell surface to ensure that a threshold can be reached, as well as a lockdown and maintenance of that state over time. The ability to establish and monitor specificity has been referred to as quality control (Boehm, 2006), and this can be broken down into the development of an effector system (education) and its maintenance over time (tolerance). Although early work in comparative immunology focused on finding evolutionary relationships between the receptors and ligands involved in histocompatibility, results over the last 5 years clearly demonstrate that they do not exist: there are no orthologous relationships between receptor-ligand pairs among the metazoa. This lack of conservation suggests that quality control is probably the basal and conserved portion of recognition of polymorphic ligands (De Tomaso, 2009).

If intracellular quality control processes are conserved, this would allow rapid evolution of the cell surface components, a convenient characteristic for an immune system. Supporting this hypothesis is the finding that nearly all phases of vertebrate immunity function through an integration of activating and inhibitory pathways through a shared set of signaling domains (e.g., ITAMs and ITIMs) and their cognate signal transduction molecules, both kinases (e.g., zap70) and phosphatases (e.g., shp 1,2). These signaling pathways are used by a diverse array of nonorthologous receptor families, and it is these components that are conserved and have been found in nearly all metazoan genomes (De Tomaso, 2009). And while there is no direct linkage between allorecognition and these signaling pathways in *Botryllus* or other nonvertebrates yet, we have shown that the discrimination of polymorphic ligands in *B. schlosseri*, a basal chordate, consists of two independent pathways: one controlling fusion and one controlling rejection. This ability is encoded in a paired receptor system consisting of a polymorphic and nonpolymorphic member that function in these two pathways, which are

in turn integrated and an outcome decided. This integration process occurs within a single epithelial layer of the extracorporeal ampullae, and this recognition system has the ability to pinpoint a self *fuhc* allele from hundreds of competing specificities.

A typical mammalian immune effector cell expresses multiple activating and inhibitory receptors and integrates numerous inputs to generate a response, but how this integration occurs is not well understood (Brodin et al., 2009; Mueller, 2003). In contrast, direct manipulation of only two proteins can recapitulate all aspects of histocompatibility in *B. schlosseri*, offering a simplified model to dissect multiple aspects of the cell biology that underlie the ability of an innate effector system to discriminate between highly polymorphic ligands.

EXPERIMENTAL PROCEDURES

Animals and Mariculture

Conditions for raising *Botryllus schlosseri* in the laboratory and the techniques for assaying phenotypic histocompatibility have been comprehensively described elsewhere (Boyd et al., 1986; Nyholm et al., 2006). Individuals were collected from harbors along the California coast, including populations from Santa Cruz, Monterey Bay, Santa Barbara, and San Diego. Additionally, several individuals were collected from Woods Hole, MA. All specimens collected outside of the Monterey Bay area were initially frozen in liquid nitrogen and subsequently stored at -80°C .

Genetic Mapping, Cloning, and Sequencing of *uncle fester*

A complete description of the genetic and physical mapping of the *fuhc* locus, DNA and RNA isolation, cDNA synthesis, DNA and protein sequence sequencing, and topological analysis can be found in the following references (Nyholm et al., 2006; De Tomaso et al., 2005; De Tomaso and Weissman, 2003). Enzymes were from NEB (Beverly, MA). All chemicals were purchased from Fisher (Pittsburgh, PA). Oligonucleotides were synthesized by Operon (Chatsworth, CA). Kits were used for specific processes as described below.

The entire *uncle fester* gene was isolated by RACE (Frohman et al., 1987) via the Smart II RACE Kit (BD) with the following primers (5'-3'): sense, GAATGTTCTACGACCGTTGGTGAT; sense nest, AACCGCTACTAGTCGCTCCGGTAAT; antisense, AAAATGGAATATCAATGAGACTTTGTG; antisense nest, CTACAACCTACCAGTGCAGAGCTGAT. Once the entire gene was sequenced, the following two primers were designed from the 5' and 3' untranslated regions to amplify the entire gene: 5' UTR, AAAACATATGATAC CAGACTGCTTACC; 3' UTR, GCAGCTGCTTCGATTTTCTTTCCTTGT. In addition, the following internal primers were designed within the coding region of *uncle fester* to verify the observed patterns of population level polymorphism: F1, TCATCCACTTGGGCGTATGACACA; and R1, ATCGCTTCCTGGCA TAAAGTCCA.

uncle fester was amplified from cDNA of wild-type and lab-reared individuals or pooled samples from different populations (Woods Hole and Sandwich Bay, MA, and San Diego, Santa Barbara, Monterey, and Santa Cruz, CA). Individual bands (arrows, Figure 2A) were isolated and subcloned, and multiple clones ($n = 48-96$) were sequenced and analyzed, revealing polymorphisms and splice variants. All possible combinations of primers were used on both pooled and individual cDNA samples to verify that identified polymorphisms were segregating in the populations.

Whole-Mount In Situ Hybridization

Whole-mount in situ hybridizations were carried out according to previously published methods (De Tomaso et al., 2005; Nyholm et al., 2006) with the following minor adjustments. Samples were fixed in 4% ultra-pure paraformaldehyde buffered with 0.5 M NaCl, 0.1 M MOPS (pH 7.5) overnight at 4°C . Embryos, tadpole larvae, juvenile oozoids, and adults were hybridized with dioxygenin-UTP-labeled probes designed to a unique portion of the *uncle fester* ectodomain. After development with BCIP/NBT, adults were embedded in paraffin and cut into 5–7 μm thick sections. The tissues were then counterstained with Eosin.

RNA Interference

RNA interference, allorecognition assays, and controls were done as previously described (Nyholm et al., 2006; also described in text). Two RNAi constructs were used. First, siRNAs covering the first 400 bp of *uncle fester* were constructed according to the directions specified by the commercially available Ambion dicer enzyme kit. In addition, Stealth siRNAs targeting the first exon of *uncle fester* were purchased from Invitrogen with the following sense sequence: 5'-CATGACATTGCATGGTCATTGCAA-3'. Both reagents could knock down *uncle fester* expression to <1% of normal levels as assessed by qPCR with no observable differences and had no effect on expression of *fester*.

Control subclones were injected with a custom designed stealth siRNA constructed to GFP, to ensure that the phenotype observed during the *uncle fester* knockdown was specific. All ampullar tissues were frozen in liquid nitrogen and stored at -80°C . Quantitative PCR analysis was performed with iQ SYBR Green Supermix (BioRad, Hercules, CA) on a BioRad iCycler Optical Module. Data was analyzed with the $2^{-\Delta\Delta\text{Ct}}$ method (Livak and Schmittgen, 2001), with elongation factor 1- α (EF1- α) as a housekeeping gene.

mAb Production, Immunofluorescence, FACS, and Direct Stimulation

Monoclonal antibodies were generated to *uncle fester* and used in whole-mount IF as described previously (Figure S2; Nyholm et al., 2006). For FACS analysis, single-cell suspensions were isolated (Laird et al., 2005), then stained with mAbs to *fester* and *uncle fester* that had been directly conjugated to fluorophores (680 and 488, respectively; Pierce, Rockford, IL) for 1 hr at 4°C with occasional mixing. The cells were centrifuged at $500 \times g$ for 10 min at 4°C , washed 2x, then resuspended and analyzed with a Guava EasyCyte 8HT (Millipore, Billerica, MA) equipped with two lasers. When comparing live unstained *Botryllus* cells to cells stained with propidium iodide, a significant overlap of autofluorescent and PI-positive cells exists, making it difficult to exclude dead cells from the analysis with only PI. Therefore, all cells were included in the analysis and gates were drawn by means of a control sort of cells stained with both secondary anti-mouse IgGs (680 and 488). This gating excludes any false-positive autofluorescent and/or dead cells.

For mAb stimulation of *Botryllus* colonies, goat anti-mouse IgG magnetic beads (NEB) were first washed 3x in PBS containing 5% BSA for 10 min, then incubated with either purified antibody (in PBS containing 3% BSA) or hybridoma supernatant for 1 hr shaking at 4°C . Magnetic beads were then delivered to the tips of the ampullae and held in place by a magnet located underneath the glass slide in which the animal was residing. The beads were applied for 15 min and the colonies were monitored for 48 hr.

SUPPLEMENTAL INFORMATION

Supplemental Information includes two figures and one table and can be found with this article online at doi:10.1016/j.immuni.2011.01.019.

ACKNOWLEDGMENTS

We thank K. Palmeri, K. Ishizuka, and M. Caun for help with animal rearing; L. Jerabek, M. Inlay, T. Serwold, and I. Weissman for help with antibody production; and J. Carlyle and N. Netuschil for critical reading of the manuscript and helpful discussions. This research was supported by NIH grants AI041588 and DK045762 to A.W.D. and EPA STAR fellowship 91631401-0 and NIH grant 1F31A1075606-01A2 to T.R.M.

Received: August 17, 2010

Revised: December 2, 2010

Accepted: January 21, 2011

Published online: April 14, 2011

REFERENCES

Azumi, K., De Santis, R., De Tomaso, A.W., Rigoutsos, I., Yoshizaki, F., Pinto, M.R., Marino, R., Shida, K., Ikeda, M., Ikeda, M., et al. (2003). Genomic analysis of immunity in a Urochordate and the emergence of the vertebrate immune system: "Waiting for Godot". *Immunogenetics* 55, 570–581.

Ballarin, L., Cima, F., and Sabbadin, A. (1995). Morula cells and histocompatibility in the colonial ascidian *Botryllus schlosseri*. *Zoolog. Sci.* 12, 757–764.

Boehm, T. (2006). Quality control in self/nonself discrimination. *Cell* 125, 845–858.

Boyd, H.C., Brown, S.K., Harp, J.A., and Weissman, I.L. (1986). Growth and sexual maturation of laboratory-cultured Monterey Bay *Botryllus schlosseri*. *Biol. Bull.* 170, 91–109.

Brodin, P., Kärre, K., and Höglund, P. (2009). NK cell education: Not an on-off switch but a tunable rheostat. *Trends Immunol.* 30, 143–149.

Burnet, F.M. (1971). "Self-recognition" in colonial marine forms and flowering plants in relation to the evolution of immunity. *Nature* 232, 230–235.

Cima, F., Sabbadin, A., and Ballarin, L. (2004). Cellular aspects of allorecognition in the compound ascidian *Botryllus schlosseri*. *Dev. Comp. Immunol.* 28, 881–889.

De Tomaso, A.W. (2009). Sea squirts and immune tolerance. *Dis Model Mech* 2, 440–445.

De Tomaso, A.W., and Weissman, I.L. (2003). Initial characterization of a protochordate histocompatibility locus. *Immunogenetics* 55, 480–490.

De Tomaso, A.W., Nyholm, S.V., Palmeri, K.J., Ishizuka, K.J., Ludington, W.B., Mitchel, K., and Weissman, I.L. (2005). Isolation and characterization of a protochordate histocompatibility locus. *Nature* 438, 454–459.

Dehal, P., Satou, Y., Campbell, R.K., Chapman, J., Degnan, B., De Tomaso, A., Davidson, B., Di Gregorio, A., Gelpke, M., Goodstein, D.M., et al. (2002). The draft genome of *Ciona intestinalis*: Insights into chordate and vertebrate origins. *Science* 298, 2157–2167.

Delsuc, F., Brinkmann, H., Chourrout, D., and Philippe, H. (2006). Tunicates and not cephalochordates are the closest living relatives of vertebrates. *Nature* 439, 965–968.

Fernandez, N.C., Treiner, E., Vance, R.E., Jamieson, A.M., Lemieux, S., and Raulet, D.H. (2005). A subset of natural killer cells achieves self-tolerance without expressing inhibitory receptors specific for self-MHC molecules. *Blood* 105, 4416–4423.

Frohman, M.A., Dush, M.K., and Martin, G.R. (1987). Rapid production of full-length cDNAs from rare transcripts; amplification using a single gene-specific oligonucleotide primer. *Proc. Natl. Acad. Sci. USA* 85, 8998–9002.

Höglund, P., and Brodin, P. (2010). Current perspectives of natural killer cell education by MHC class I molecules. *Nat. Rev. Immunol.* 10, 724–734.

Joncker, N.T., Fernandez, N.C., Treiner, E., Vivier, E., and Raulet, D.H. (2009). NK cell responsiveness is tuned commensurate with the number of inhibitory receptors for self-MHC class I: The rheostat model. *J. Immunol.* 182, 4572–4580.

Kärre, K., Ljunggren, H.G., Piontek, G., and Kiessling, R. (1986). Selective rejection of H-2-deficient lymphoma variants suggests alternative immune defence strategy. *Nature* 319, 675–678.

Kim, S., Poursine-Laurent, J., Truscott, S.M., Lybarger, L., Song, Y.J., Yang, L., French, A.R., Sunwoo, J.B., Lemieux, S., Hansen, T.H., and Yokoyama, W.M. (2005). Licensing of natural killer cells by host major histocompatibility complex class I molecules. *Nature* 436, 709–713.

Laird, D.J., De Tomaso, A.W., and Weissman, I.L. (2005). Stem cells are units of natural selection in a colonial ascidian. *Cell* 123, 1351–1360.

Lanier, L.L. (2001). Face off—The interplay between activating and inhibitory immune receptors. *Curr. Opin. Immunol.* 13, 326–331.

Litman, G.W., Rast, J.P., and Fugmann, S.D. (2010). The origins of vertebrate adaptive immunity. *Nat. Rev. Immunol.* 10, 543–553.

Livak, K.J., and Schmittgen, T.D. (2001). Analysis of relative gene expression data using real-time quantitative PCR and the $2^{-\Delta\Delta\text{Ct}}$ method. *Methods* 25, 402–408.

Mueller, D.L. (2003). Tuning the immune system: Competing positive and negative feedback loops. *Nat. Immunol.* 4, 210–211.

Nagashima, L., and Scofield, V.L. (1981). The studies of the rejection reaction in botryllus oozoids. *Am. Zool.* 21, 984.

Nyholm, S.V., Passegue, E., Ludington, W.B., Voskoboinik, A., Mitchel, K., Weissman, I.L., and De Tomaso, A.W. (2006). Isolation and characterization of *fester*, a candidate allorecognition receptor from a primitive chordate. *Immunity* 25, 163–173.

- Rinkevich, B., Porat, R., and Goren, M. (1995). Allorecognition elements on a urochordate histocompatibility locus indicate unprecedented extensive polymorphism. *Proc. R. Soc. Lond.* 259, 319–324.
- Rinkevich, B., Tartakover, S., and Gershon, H. (1998). Contribution of morula cells to allogeneic responses in the colonial urochordate *Botryllus schlosseri*. *Mar. Biol.* 131, 227–236.
- Scofield, V.L., and Nagashima, L.S. (1983). Morphology and genetics of rejection reactions between oozodis from the tunicate *Botryllus schlosseri*. *Biol. Bull.* 165, 733–744.
- Scofield, V.L., Schlumpberger, J.M., West, L.A., and Weissman, I.L. (1982). Protochordate allorecognition is controlled by a MHC-like gene system. *Nature* 295, 499–502.